ELSEVIER

Thermochimica Acta 266 (1995) 231–238

thermochimica acta

Adiabatic calorimetric study on shape memory alloys: heat capacities and martensitic phase transformation of $Ni_{47}Ti_{44}Nb_9$ and $Nb_{80}Ti_{14}Ni_6$ alloys ☆

Guang-Yu Sun [a], Zhi-Cheng Tan [a,*], Yi-Sun [a], Guan-Jun Yang [b], Shi-Ming Hao [c]

[a] *Dalian Institute of Chemical Physics, Academia Sinica, Dalian 116023, People's Republic of China*
[b] *Titanium Alloy Institute, Northwest Institute for Non-ferrous Metal Research, Baoji 721014, Shaanxi, People's Republic of China*
[c] *Department of Material Science and Engineering, Northeastern University, Shenyang 110006, People's Republic of China*

Abstract

A low-temperature precision adiabatic calorimeter for heat capacity measurements has been constructed. The heat capacities of a shape memory alloy ($Ni_{47}Ti_{44}Nb_9$) and a normal reference alloy ($Nb_{80}Ti_{14}Ni_6$) have been measured in the temperature range from 60 to 350 K with this calorimeter. The heat capacity curve of the normal alloy is smooth and continuous over the whole temperature range. An anomaly, indicating the martensitic phase transformation, in the heat capacity curve of the shape memory alloy was observed at $T = 234.0 \pm 0.5$ K with a maximum, where $C_{p,m} = 34.86 \pm 0.21$ J K^{-1} mol^{-1}. The molar enthalpy and molar entropy associated with the martensitic transformation were determined as $\Delta_{trs}H_m^\circ = 411.9 \pm 2.5$ J mol^{-1} and $\Delta_{trs}S_m^\circ = 1.76 \pm 0.01$ J K^{-1} mol^{-1}, respectively.

Keywords: Adiabatic calorimetry; Heat capacity; Martensitic phase transformation; Shape memory alloy

1. Introduction

The shape memory effect (SME) has received increasing attention in recent decades, because shape memory alloys (SMA) have been widely used as new functional materials

* Corresponding author.
☆ Dedicated to Hiroshi Suga on the Occasion of his 65th Birthday.

0040-6031/95/$09.50 © 1995 – Elsevier Science B.V. All rights reserved
SSDI 0040-6031(95)02438-7

with commercial applications in pipe couplings, electrical connectors, various actuators, medical appliance, etc. The shape memory effect is one of the effects associated with martensitic phase transformations [1–3] induced by stress or thermal treatment. These effects include thermoelasticity, pseudoelasticity, SME and the two-way shape memory effect. After a material is deformed by application of a stress at one temperature, the shape memory effect arises when it recovers its original shape during heating to a higher temperature instead of removing the stress. Many alloy systems such as CuZnAl [4], TiPd [5], FePt [6] and TiNi [7–10] show SME, and TiNi alloy is the most widely used SMA because of its excellent mechanical properties among these systems.

Martensitic transformation proceeds in equilibrium between the chemical and non-chemical driving forces. These two kinds of forces can be evaluated separately in a quantitative way using heat capacity data [11], so that more information concerning the martensitic phase transformation can be obtained. Although differential scanning calorimetry has been used to measure the heat capacities of SMA [12] as well as to determine the transformation temperatures [5, 13, 14], no research work on SMA by adiabatic calorimetry has been reported until now. For this purpose we have constructed an adiabatic calorimeter, and measured the heat capacities of a shape memory alloy and a reference alloy in the temperature range from 60 to 350 K using this calorimeter. On the basis of the heat capacity measurements, the molar enthalpy and molar entropy associated with the martensitic transformation of the investigated SMA were determined.

2. Experimental

2.1. Materials and preparation of alloy samples

Samples of the two alloys studied were prepared by the conventional vacuum induction melting technique. Titanium (purity, 99.8%), nickel (purity, 99.9%) and niobium (purity, 99.9%) were remelted in a graphite crucible and cast in vacuum. The ingots were homogenized at 800°C for 24 h in an argon atomosphere and then quenched in water. Then, they were machined to a cylinder 20 mm in diameter for the heat capacity measurements. The atomic compositions of the alloys prepared were $Ni_{47}Ti_{44}Nb_9$ for the shape memory alloy (SMA) sample and $Nb_{80}Ti_{14}Ni_6$ for the reference alloy sample. Measured by a four-wire electrical resistance method prior to the heat capacity measurements, the transformation temperatures of the SMA sample were found to be as follows: $M_s = 170\,K$, $M_f = 148\,K$, $A_s = 225\,K$ and $A_f = 251\,K$, where M_s and M_f are the start and finish temperatures of a forward martensitic transformation, and A_s and A_f are the start and finish temperatures of a reverse martensitic transformation.

2.2. Construction of the adiabatic calorimeter

The heat capacity measurements of the two alloys were performed by a low-temperature adiabatic calorimeter. The construction of the cryostat of the calorimeter is similar to that described elsewhere [15]. The alloy sample, sealed in a sample cell and

surrounded by two adiabatic shields, was housed in a high vacuum and immersed in liquid nitrogen. The two adiabatic shields were made of chromium-plated copper (0.5 mm thick) and equipped with manganin heating wires (0.2 mm in diameter). The inner shield, which is a little smaller than the outer one, was hung from the top of the outer one by three pieces of fine nylon thread, while the outer shield was hung from the top of the vacuum can by the same means. Two sets of six-junction chromel–copel (Ni 55%; Cu, 45%) thermocouples were used to indicate the temperature differences between the sample cell and the inner adiabatic shield, and between the inner and the outer shields. The temperature of the two shields were controlled separately with two sets of autoadiabatic controllers operating in PID mode. The principle of the automatic adiabatic control circuitry was described in detail previously [15, 16]. The vacuum can was evacuated to about 1×10^{-3} Pa by an oil diffusion pump system during heat capacity measurements. A mechanical pump was used to pump out the nitrogen vapour from the Dewar vessel to solidify the remaining liquid nitrogen, and then 60 K or an even lower temperature was obtained.

The sample cell, shown in Fig. 1, was made of gold-plated copper (0.3 mm wall thickness) with an internal volume of 6.3 cm^3. On the side surface of the cell, a heater of Karma wires (0.15 mm in diameter, $R \approx 105\Omega$) was wound bifilarly and fixed with

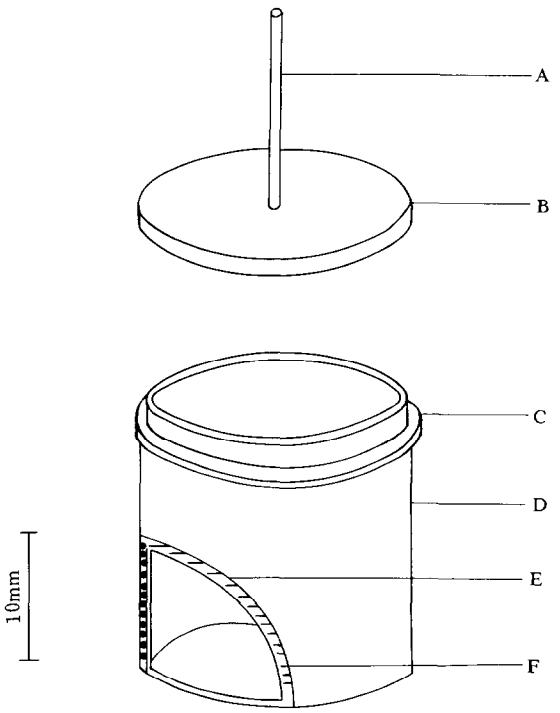

Fig. 1. Sample cell of the calorimeter: A, copper capillary; B, gold-plated silver lid; C, sealing flange; D, main body of the sample cell; E, aluminium-plated dacron film; F, heating wires.

a special cycloweld, and covered with a piece of aluminium-plated dacron film. A copper sheath was silver-soldered on the bottom of the cell to contain a miniature platinum resistance thermometer. The thermometer (Model IPRT, No. 2, SIAM Co., 15 mm long, 1.5 mm in diameter, $R_0 = 100\,\Omega$) was calibrated in terms of ITS-90 at the Centre of Low-Temperature Metrology and Measurements, Academia Sinica, in the temperature range 50–400 K with an uncertainty of about 1 mK. A gold-plated copper lid with a length of copper capillary was sealed to the sample cell using a small amount of the cycloweld. After the alloy sample was loaded in the cell, 0.1 MPa helium gas was introduced to the cell through the capillary to facilitate thermal equilibrium, and then the capillary was pinched off. The sample cell was hung from the top of the inner adiabatic shield by a length of nylon thread through a hook made by the capillary. The apparatus for temperature and energy measurement used in this calorimeter are the same as used in our previous work [16].

2.3. Experimental procedure

The alloy sample, sealed in the sample cell, was first cooled down to the lowest temperature (about 55 K which is the lower limit of the temperature that the calorimetric system can reach) and kept at this temperature for half an hour. The heat capacity measurements as a function of temperature in the heating direction using the standard discrete heating method were then initiated. In this intermittent mode, the sequence of heat capacity measurements were composed of two successively alternating periods. One was "the drift period" during which the temperature of the calorimeter cell was observed as a function of time. The other was "the energy input period" during which a definite amount of electrical energy was supplied to the calorimeter cell. The supplied energy was determined on the basis of measurements of voltage and current across and through the heater of the sample cell as well as the interval of energy input. The cycles of measurements for temperature and energy input were repeated in the above sequence until the upper limit of the temperature (about 350 K) for the measurements had been reached. In our experiments the duration of energy input was 10 min, and the thermal equilibrium inside the sample cell was attained within 3–5 min after the energy input. The temperature increment for each experimental point was about 3 K in the whole temperature range from 60 to 350 K.

3. Results and discussion

3.1. Heat capacities of α-Al_2O_3

In order to assess the precision and the accuracy of the present calorimeter, heat capacity measurements on the standard reference material α-Al_2O_3 were made before the measurements on the alloy samples. The α-Al_2O_3 sample was a spectroscopically pure reagent with a purity of 99.993 wt%. XRD analysis showed that the whole sample was in the α-phase. The mass of the α-Al_2O_3 sample used for the measurements amounted to 8.7353 g (0.085673 mol, based on a molar mass of 101.9613 g mol^{-1}). The

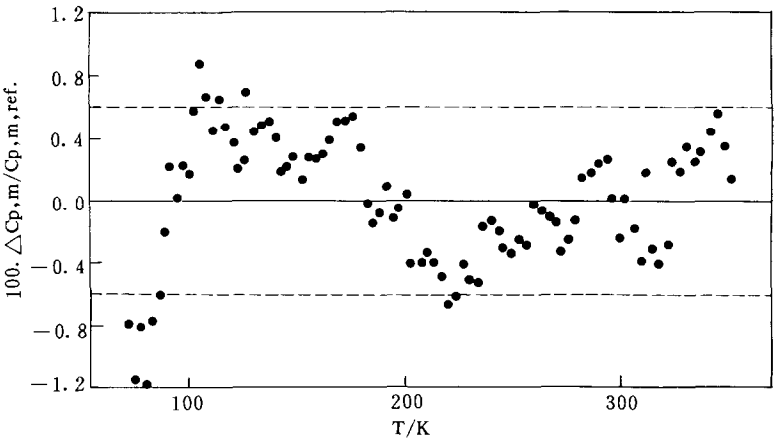

Fig. 2. Plot of deviations $100 \times (\Delta C_{p,m}/C_{p,m,ref})$ of the experimental values for the molar heat capacity of α-Al_2O_3, where $C_{p,m,ref}$ is the molar heat capacity regarded as the reference value given by Ditmars et al. [17], and $\Delta C_{p,m}$ is the difference between our value and $C_{p,m,ref}$.

Table 1
Experimental molar heat capacity of shape memory alloy; $M(Ni_{47}Ti_{44}Nb_9) = 57.0160$ g mol^{-1}

T/K	$C_{p,m}$/ J K^{-1} mol^{-1}	T/K	$C_{p,m}$/ J K^{-1} mol^{-1}	T/K	$C_{p,m}$/ J K^{-1} mol^{-1}	T/K	$C_{p,m}$/ J K^{-1} mol^{-1}
62.664	8.399	133.144	18.507	209.594	25.252	275.881	26.746
65.776	9.047	136.426	18.832	213.198	26.301	279.718	26.614
68.863	9.666	139.849	19.071	216.609	27.468	283.578	26.570
71.951	10.262	143.414	19.369	219.854	29.029	287.447	26.516
75.158	10.870	146.926	19.605	222.928	30.557	291.291	26.475
78.498	11.484	150.397	19.836	225.836	32.416	295.107	26.431
81.764	12.078	153.824	20.098	228.633	33.581	298.922	26.399
85.131	12.651	157.347	20.313	231.323	34.450	302.739	26.363
88.603	13.247	160.968	20.557	233.999	34.854	306.543	26.367
92.050	13.779	164.549	20.789	236.642	34.509	310.345	26.371
95.601	14.317	168.162	21.014	239.333	33.624	314.144	26.378
99.213	14.838	171.811	21.237	242.084	32.794	317.944	26.386
102.780	15.313	175.500	21.440	244.905	31.784	321.750	26.395
106.377	15.736	179.228	21.673	247.822	30.945	325.550	26.408
110.010	16.162	182.997	21.928	250.845	30.091	329.339	26.422
113.539	16.594	186.805	22.130	253.553	29.025	333.109	26.437
116.961	16.977	190.566	22.379	257.120	28.270	336.867	26.453
120.296	17.277	194.367	22.729	260.485	28.050	340.614	26.469
123.567	17.619	198.192	23.114	264.024	27.690	344.347	26.485
126.775	17.970	202.020	23.625	267.769	27.441	348.073	26.501
129.926	18.208	205.849	24.273	272.067	27.024	351.813	26.519

measured $C_{p,m}$ values were fitted to a sixth-degree polynomial. The overall precision of this calorimeter was ± 0.2%, as evaluated from the deviations of the experimental $C_{p,m}$ values from the sixth-degree polynomial. Fig. 2 shows the deviations of the measured molar heat capacities of α-Al_2O_3 from the recommended values measured by Ditmars et al. [17]. Expect for some points near 110 K, our results agreed with the literature values within ± 0.6%, as shown in the plot.

3.2. *Heat capacities of SMA and RA*

The experimental molar heat capacities of the shape memory alloy ($Ni_{47}Ti_{44}Nb_9$) and the reference alloy ($Nb_{80}Ti_{14}Ni_6$) samples are listed in Tables 1 and 2, respectively. The masses of the samples used in heat capacity measurements were 38.9340 g (0.68286 mol) for SMA and 23.9619 g (0.28340 mol) for RA. The molar masses of the substances investigated in this paper were calculated based on the Standard Atomic Weights of Elements 1991 [18]. The temperature range of measurements covered 60–350 K for both alloy samples. The heat capacity of the samples represented 79% of the measured total heat capacity at 60 K to 82% at 350 K for SMA, and 67 to 64% for RA. The temperature increment due to each energy input was small enough to permit the curvature correction to be ignored in comparison with the experimental error.

Table 2
Experimental molar heat capacity of the reference alloy; $M(Nb_{80}Ti_{14}Ni_6) = 84.5503$ g mol^{-1}

T/K	$C_{p,m}$/ J K^{-1} mol^{-1}	T/K	$C_{p,m}$/ J K^{-1} mol^{-1}	T/K	$C_{p,m}$/ J K^{-1} mol^{-1}	T/K	$C_{p,m}$/ J K^{-1} mol^{-1}
59.362	10.120	133.819	20.213	209.469	23.262	288.168	24.758
61.260	10.605	137.370	20.421	213.168	23.340	291.916	24.816
63.437	11.118	140.859	20.622	216.847	23.416	295.616	24.876
66.003	11.665	144.353	20.891	220.502	23.492	299.326	24.942
69.238	12.313	147.909	21.045	224.131	23.568	303.053	25.002
73.208	13.076	151.483	21.228	227.741	23.643	306.837	25.056
77.662	13.872	155.021	21.421	231.342	23.717	310.675	25.117
82.134	14.658	158.580	21.567	234.928	23.791	314.508	25.180
86.552	15.374	162.212	21.740	238.448	23.865	318.338	25.233
90.787	16.017	165.867	21.853	242.072	23.938	322.160	25.296
94.701	16.582	169.495	22.015	245.821	24.011	325.976	25.357
98.505	17.062	173.097	22.180	249.735	24.082	329.786	25.414
102.242	17.577	176.673	22.311	253.636	24.153	333.592	25.472
105.955	17.976	180.279	22.414	257.526	24.224	337.397	25.539
109.516	18.312	183.918	22.523	261.392	24.294	341.190	25.601
112.958	18.555	187.534	22.661	265.230	24.363	344.971	25.656
116.380	18.867	191.181	22.779	269.075	24.432	348.742	25.720
119.788	19.237	194.864	22.868	272.935	24.501	352.498	25.778
123.229	19.444	198.529	22.980	276.766	24.568		
126.712	19.721	202.173	23.064	280.581	24.635		
130.242	19.973	205.802	23.166	284.381	24.701		

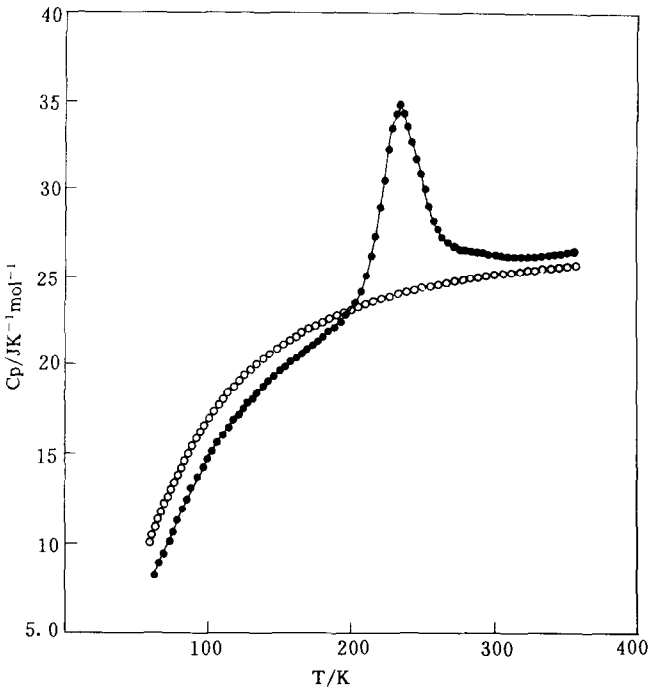

Fig. 3. Measured molar heat capacities of SMA and RA. ●, SMA ($Ni_{47}Ti_{44}Nb_9$); ○, RA ($Nb_{80}Ti_{14}Ni_6$).

A plot of the experimental values of $C_{p,m}$ versus T is shown in Fig. 3. From the figure, it can be seen that the curve of $C_{p,m}$ vs. T for RA sample is completely smooth, with no sign of any phase transformation or other thermal anomaly in the whole temperature range between 60 and 350 K. The curve of $C_{p,m}$ vs. T for SMA, however, clearly shows a thermal anomaly which is associated with the martensitic phase transformation. The heat capacity anomaly corresponding to the martensitic transformation began at approx. 209 K, reached its maximum at (234.0 ± 0.5) K with a value of $C_{p,m} = (34.86 \pm 0.21)$ J K^{-1} mol^{-1}, and ended at approx. 265 K, respectively. Assuming that the normal heat capacity in the transition temperature region was approximated by the smoothed interpolating curve, the molar enthalpy and the molar entropy associated with the martensitic transformation were determined as $\Delta_{trs}H_m^\circ = 411.9 \pm 2.5$ J mol^{-1} and $\Delta_{trs}S_m^\circ = 1.76 \pm 0.01$ J K^{-1} mol^{-1}, respectively, by graphical integration of the excess heat capacities.

Acknowledgement

The authors are grateful to the National Natural Science Foundation of China for providing financial support to this research project under the grant No. 29170152.

References

[1] L. Delaey, R.V. Krishnan, H. Tas and H. Warlimont, J. Mater. Sci., 9 (1974) 1521.
[2] R.V. Krishnan, L. Delaey, H. Tas and H. Warlimont, J. Mater. Sci., 9 (1974) 1536.
[3] H. Warlimont, L. Delaey, R.V. Krishnan and H. Tas, J. Mater. Sci., 9 (1974) 1545.
[4] T. Xiao, G.P. Johari and C. Mai, Metall. Trans. A, 24 (1993) 2743.
[5] K. Otsuka, K. Oda, Y. Ueno, M. Piao, T. Ueki and H. Horikawa, Scr. Metall. Mater., 29 (1993) 1355.
[6] K. Takezawa, S. Sato, K. Minato, S. Maruyama and K. Marukawa, Mater. Trans. JIM, 33 (1992) 294.
[7] P. Filip and K. Mazanec, Scr. Metall. Mater., 30 (1994) 67.
[8] W. Tang and R. Sandstrom, Mater. Design, 14 (1993) 103.
[9] M. Piao, S. Miyazaki and K. Otsuka, Mater. Trans, JIM, 33 (1992) 346.
[10] M. Piao, S. Miyazaki, K. Otsuka and N. Nishida, Mater. Trans. JIM, 33 (1992) 337.
[11] J. Ortin and A. Planes, Acta Metall., 36 (1988) 1873.
[12] L. Manosa, A. Planes, J. Ortin and B. Martinez, Phys, Rev. B, 48 (1993) 3611.
[13] A. Takei, A. Ishida and S. Miyazaka, in H. Henein and T. Oki (Eds.), 1st Int. Conf. Process. Mater. Prop., 1993, p. 1177.
[14] F.J. Gil and J.M. Guilemany, Mater. Res. Bull., 27 (1992) 117.
[15] Tan Zhi-cheng, Zhou Li-xing, Chen Shu-xia, Yin An-xue, Sun Yi, Ye Jin-chun and Wang Xiu-kun, Sci. Sinica (Ser. B), 26 (1983) 1014.
[16] Tan Zhi-cheng, Yin An-xue, Chen Shu-xia and Zhou Li-xing, Science in China (Ser. B), 34 (1991) 560.
[17] D.A. Ditmars, S. Ishihara, S.S. Chang, G. Berstain and E.D. West, J. Res. Natl. Bur. Stand., 87 (1982) 159.
[18] Atomic Weights of Elements 1991, Pure Appl. Chem., 64 (1992) 1519.